ROZPRAWY INŻYNIERSKIE · ENGINEERING TRANSACTIONS · 31, 2, 203—211, 1983
Polska Akademia Nauk · Instytut Podstawowych Problemów Techniki

EXPERIMENTAL STUDY OF CRACKED KNEE OF FRAME

H. P. ROSSMANITH and R. J. BEER (VIENNA)

Fracture mechanics and photoelastic methods are utilized to determine correction functions for stress intensity factors for cracked knees of frame. A simple engineering method of analysis is demonstrated.

1. Introduction

During the past two decades fracture mechanics has evolved to a subject of widespread interest and its applications to engineering problems have been rapidly expanding. Mechanical and civil engineering applications of the method of fracture mechanics form the bulk of technical reports published in the literature. A wide class of fracture research contributions pertains to the determination of stress intensity factors, K, for complicated structural components with cracks. Lately, special attention has been focussed on photomechanical evaluation of stress fringe patterns for the determination of geometry-induced correction functions to the stress intensity factor.

In this contribution linear-elastic fracture mechanics in conjunction with stress-coating is utilized to determine load limits and stress intensity correction functions for cracked knees of frame in structural frameworks. The stress analyses employed base on an engineering approach [1] and a photoelastic multiparameter-multipoint data reduction method developed recently [2, 3].

2. Experimental investigation

The test program involved two series of tests with noncracked and cracked structural components. The specimen geometry to be tested and analyzed is shown in Fig. 1a. In the first test three models of a knee of frame fabricated from commercially available aluminium have a machined symmetrical edge crack of depth $a = 4$ mm on the tension (inner) side of the frame (Fig. 1a). The opening angle of the knee is 90 degrees; all dimensions are kept the same for models No 1, No 2, and No 3, except for the radius of curvature, r_i, of the re-entrant corner which varied from $r_1 = 20$ mm, $r_2 = 9$ mm to $r_3 = 4$ mm for the models No 1, No 2 and No 3, respectively. All cracks were milled with a cutter of thickness 0.5 mm.

For reference, the second test series pertained to the state of stress in the uncracked models. The uncracked test samples were fabricated of

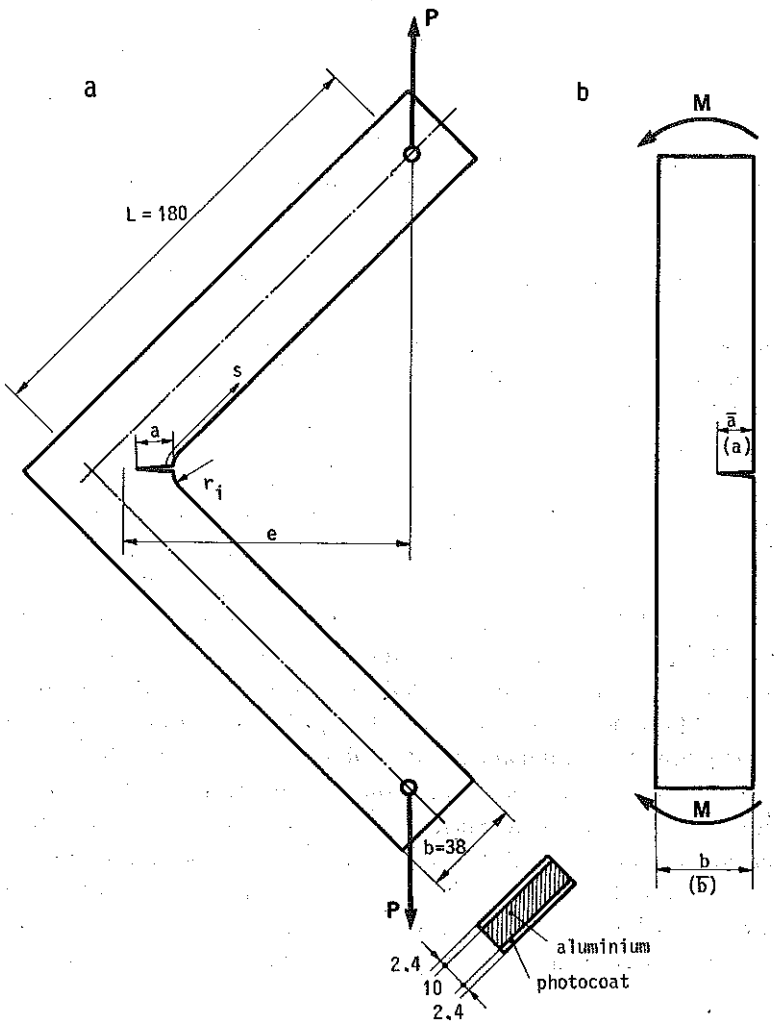

FIG. 1. Geometry and load configuration; a) structural component, b) edge-cracked strip subjected to pure bending.

Araldite B, a commercially available transparent temporarily birefringent polymer. Except for the cracks, these models have the same shape and dimensions as the cracked specimens. Unflawed Araldite models were utilized in order to increase the stress-optical effect; the precracked specimens had to be machined from aluminium and stress-coat tested because similar Araldite models failed at loads too low for any appreciable stress-induced optical effect required for fracture mechanics applications.

2.1. Testing of uncracked specimens

An important factor in the discussion of a cracked structural component is the knowledge of the stress distribution in the unflawed component.

Since the principal stress component in a direction normal to the inner boundary σ_n is zero, the photoelastic fundamental relation [4]

$$2\tau_m = \sigma_t - \sigma_n = Nf_\sigma/h \tag{2.1}$$

yields $\sigma_t = Nf_\sigma/h$. The distribution of $\sigma_t \sim N$ along the inner boundary is shown in Fig. 2. The results show a sharp increase by a factor of

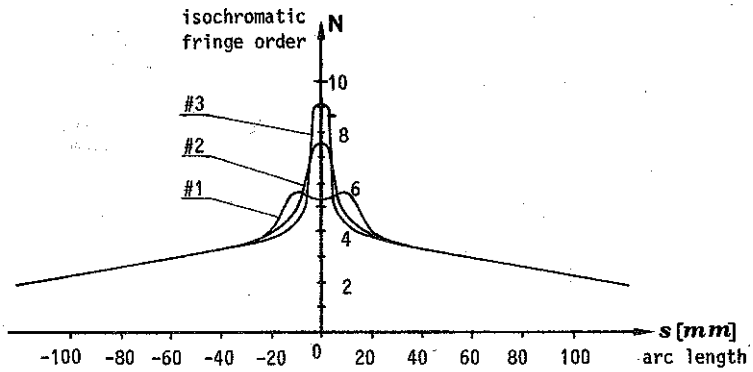

FIG. 2. Distribution of principal stress σ_t along the inner boundary of the knee of frame.

about 2 of the tangential stress σ_t at the notch root when the root radius was decreased by a factor of 5. Moreover, the section of local stress amplification is reduced from $-15 < s < 15$ {mm} (No 1) to $-5 < s < 5$ {mm} (No 3) measured with respect to the fringe order $N = 5$. Figure 2 also implies the existence of a limiting ratio $(r/b)_{\text{lim}}$, such that, for $(r_i/b) > (r/b)_{\text{lim}}$, the maximum fiber stress does not occur at the notch bottom but is attained at two points off the line of symmetry.

2.2. *Testing of precracked specimens*

The series of precracked aluminium models were then sandwiched between adhesively cemented photocoat layers of thickness 2.4 mm for isochromatic fringe pattern recording by means of an optical reflection polariscope arrangement as shown in Fig. 3. The tension load was applied by a stiff servo-hydraulic deformation-controlled testing machine. When the aluminium part of the model is subjected to tension loads, P, the photocoat-layer is accordingly strained to induce isochromatic fringes when viewed in a reflexion polariscope optical arrangement. Continuous in-plane strain deformations across the aluminium stress-coat interface forms the basis of this method expressed by [5]

$$(\varepsilon_1 - \varepsilon_2)_{\text{Alu}} = (\varepsilon_1 - \varepsilon_2)_{\text{coat}} = N\frac{\lambda}{2dc}, \tag{2.2}$$

where λ is the wave length of the monochromatic light employed ($63.5 \cdot 10^{-6}$ cm), c is a dimensionless stress-optic figure of merit ($c = 0.15$), and d is the thickness of the coating.

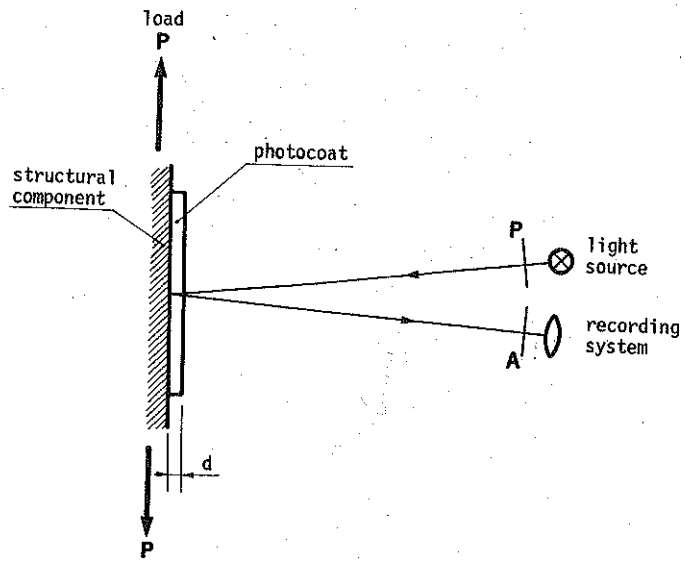

FIG. 3. Experimental set-up for isochromatic fringe pattern recording by means of reflection polariscope arrangement.

3. ANALYSIS

During the past two decades efficient methods for the determination of stress intensity factors have been developed; these are reviewed in a recent paper by ROSSMANITH and CHONA [2]. Irwin's classical engineering method

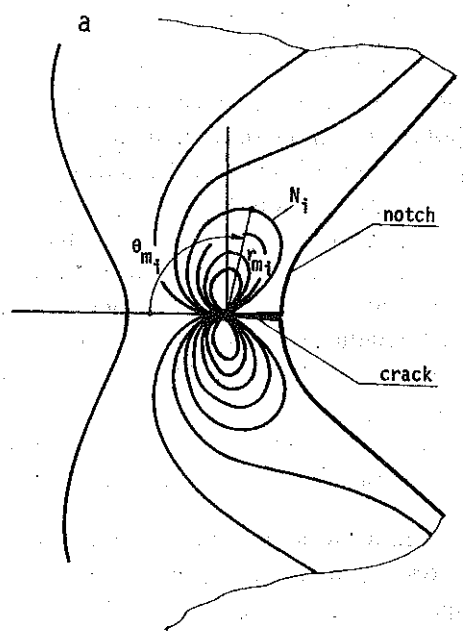

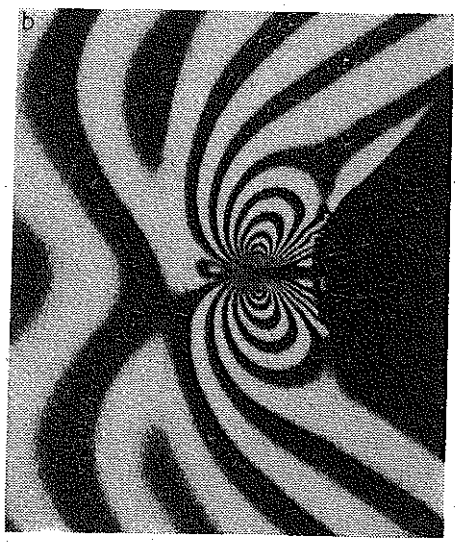

FIG. 4. Crack-tip fringe loop geometry; a) measurement quantities, b) experimentally recorded isochromatic fringe pattern (model 2).

which bases on two characteristic geometrical quantities of the isochromatic loop, tilt angle θ_m, and apogee distance, r_m (see Fig. 4a), yields for the stress intensity factor, K_1

$$K_1 = 2\tau_m \sqrt{2\pi r_m}\, H(\theta_m), \tag{3.1}$$

where the function $H(\theta_m)$ is given in Fig. 5 [6, 7].

Regarding Eq. (2.2) and the relation

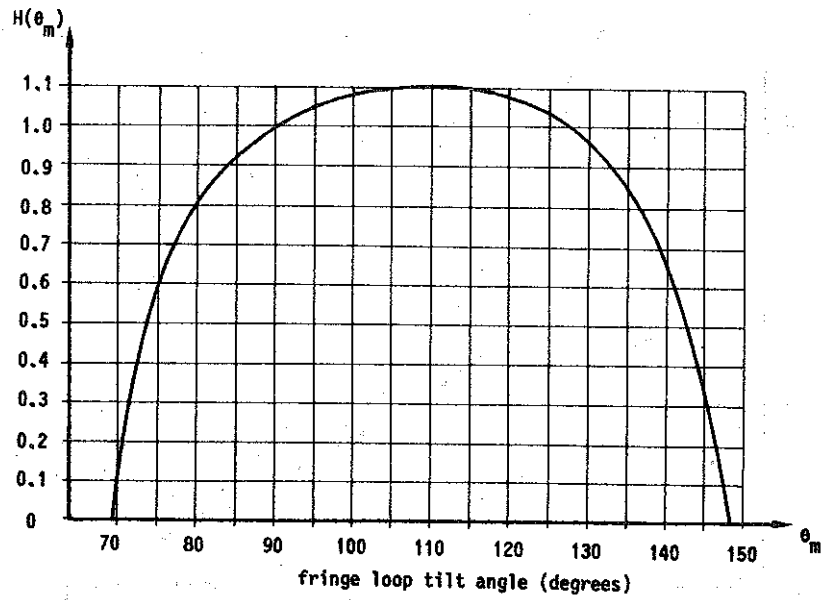

FIG. 5. Graph $H(\theta_m)$ vs. θ_m for K-determination.

$$(\varepsilon_t - \varepsilon_n) = \frac{1+\nu}{E}(\sigma_t - \sigma_n) = \frac{1+\nu}{E} 2\tau_m, \tag{3.2}$$

one obtains

$$\tau_m = \frac{E}{2(1+\nu)} \frac{\lambda}{2dc} N, \tag{3.3}$$

where Poisson's ratio $\nu = 1/3$ and Young's modulus $E = 6.5 \cdot 10^5$ kp/cm^2.

Values of r_m and θ_m as a function of the fringe order $N = 1, \ldots, 7$ for the three models No 1, No 2 and No 3 have been measured from photographic fringe pattern recordings and are reproduced in Fig. 6. A typical mode 1 isochromatic crack-tip fringe pattern associated with the model 2 is shown in Fig. 4b.

The influence of the geometrical configuration of the knee of frame, in particular the root radius, r, on the tilt of the tested isochromatic fringe follows from Fig. 6.

Combination of Eqs. (3.1) and (3.3) yields the final relation for the experimental determination of the stress intensity factor

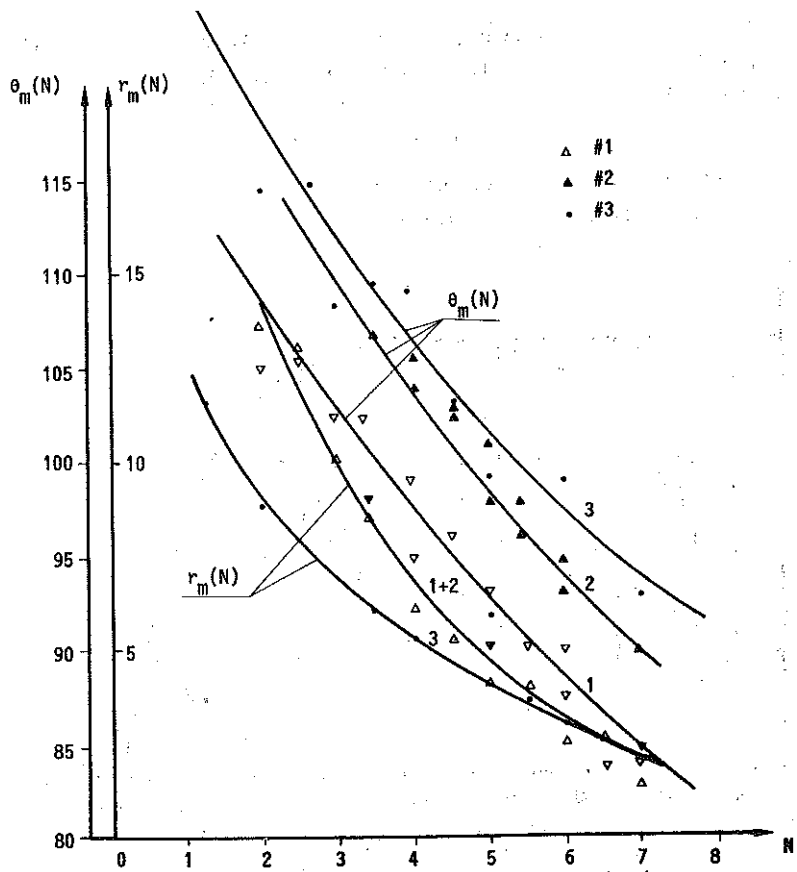

FIG. 6. Fringe measurement data for K-evaluation.

(3.4) $$K_1 = \frac{E}{1+\nu}\frac{\lambda}{2dc} N\sqrt{2\pi r_m}\, H(\theta_m).$$

4. Results and discussion

From a K-determination point of view it appears advantageous to compare the geometrical configuration of the knee of frame with the problem of an edge-cracked strip of width b and crack length, $\bar{a}$, subjected to pure bending, M (Fig. 1b), for which the stress intensity factor is given by [8]

(4.1) $$K_{1b} = \frac{6M}{b^2}\sqrt{\pi a}\, Y_b(a/b).$$

For the problem at hand a similar expression for K may be written:

(4.2) $$K_1 = \frac{6M_1}{b^2}\sqrt{\pi a}\, Y\left(\frac{a}{b}, \frac{r}{b}\right)$$

with

(4.3) $$M_1 = \mathrm{PL}/\sqrt{2} \cong \mathrm{Pe}.$$

The geometry correction factor $Y(a/b; r/b)$ has been plotted in Fig. 7 for the varying root radius r. The geometry of the knee, in particular the radius of curvature, r, induces a pronounced increase of the stress intensity factor for decreasing values of r/b. If this configuration the correction

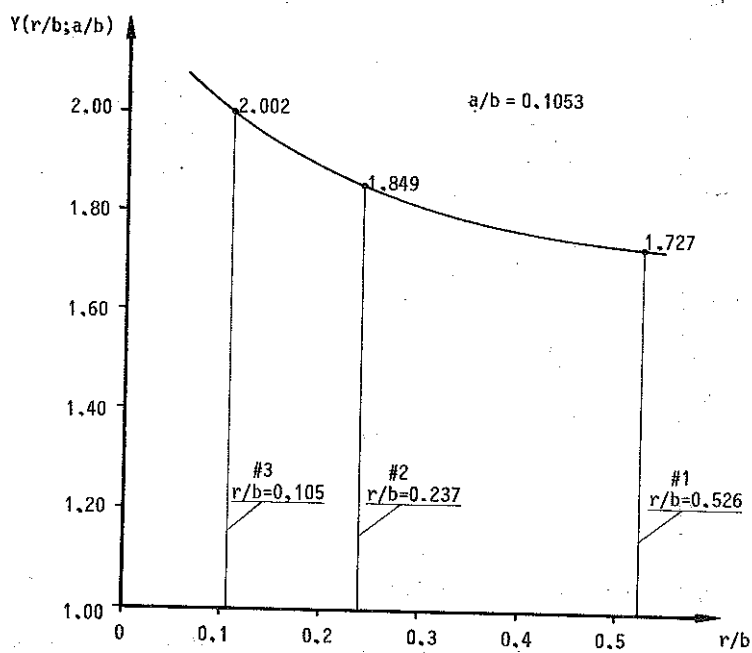

FIG. 7. Stress intensity correction function $Y(a/b; r/b)$ for a cracked knee of frame.

function, $Y(a/b, r/b)$, for the frame knee is compared with the correction function for the edge-cracked bending strip, $Y(a/b)$ [8], an effective crack length $\bar{a}$ may be evaluated to show that the flawed knee of frame is more sensitive to cracking than the edge-cracked strip configuration. Curve $\bar{a}/b$ in Fig. 8 shows the distribution of effective crack length as a function of r/b.

With regard to stress distribution and stress flow in the knee section of the structural component considered, it is tempting to introduce an "effective" strip width $\bar{b}$, such that

$$Y_b(a/\bar{b}) = Y(a/b; r/b). \tag{4.4}$$

The graph of $\bar{b}/b$ as a function of r/b is plotted in Fig. 8.

It should be noted that an engineering estimate of the tensile stress loading of the frame in the order of 5% of the bending loading has been neglected with reference to experimental error bounds.

Most recently, multiparameter-multipoint data reduction schemes have been developed on the basis of an overdetermined system of nonlinear algebraic equations solved by means of a Newton–Raphson procedure and the method of least squares [2, 3]. The isochromatic fringe patterns obtained in these tests have been analyzed by using a six-parameter method [3] and the

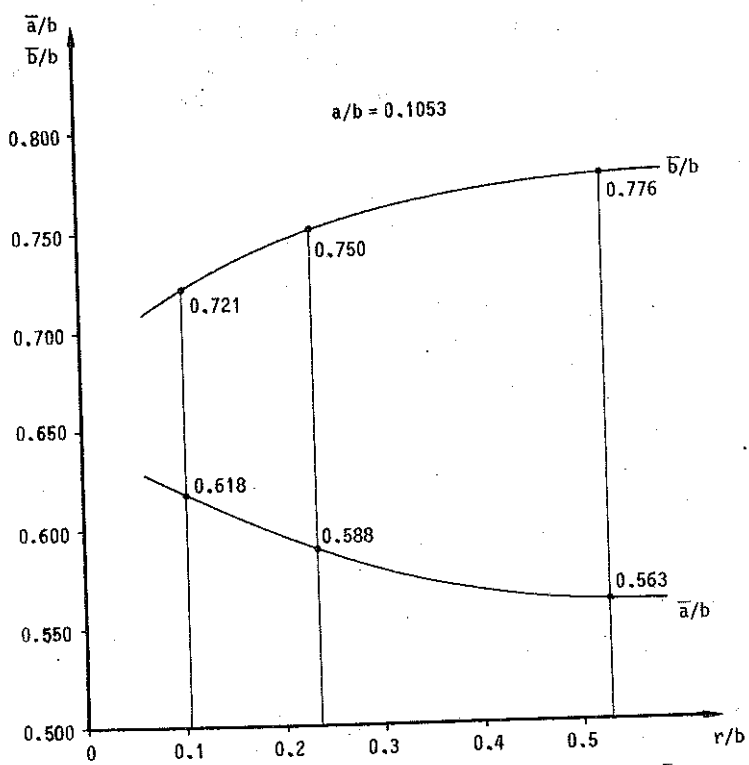

FIG. 8. Effective crack length ratio, $\bar{a}/b$, and effective strip width ratio, $\bar{b}/b$, as a function of the root radius ratio r/b.

results obtained were within a 5%-error bound with the engineering approximation presented herein.

Acknowledgment

This research program was kindly supported by the Fonds zur Förderung der wissenschaftlichen Forschung in Austria under project 3288.

References

1. G. R. Irwin, Discussion to a paper by D. Post and A. A. Wells, SESA Proc. XVI, 93–96, 1958.
2. J. W. Dally nd . J. Sanford, *Classification of stress intensity factors from isochromatic fringe patterns*, Exp. Mech., **18**, 2, 441–448, 78.
3. H. P. Rossmanith nd R. Chona. *A survey of recent developments in the evaluation of stress intensity factors from isochromatic crack-tip fringe patterns*, ICF 5, V, 2507–2516, 1981.
4. J. W. Dally and W. F. Riley, *Experimental stress analysis*, McGraw-Hill, 1978.
5. F. Zandman, S. Redner and J. W. Dally, *Photoelastic coatings*, SESA Monograph, 3, 1977.
6. H. P. Rossmanith and G. R. Irwin, *Analysis of dynamic isochromatic crack-tip stress patterns*. University of Maryland. Department of Mechanical Engineering Report, 443, 1979.
7. O. C. Zienkiewicz, *A new look at the Newmark, Haubolt and other time stepping formulas. factors from isochromatic crack-tip fringe patterns*, J. Appl. Mech., **47**, 795–800, 1980.
8. H. Tada, P. C. Paris and G. R. Irwin, *The stress analysis of cracks*, Handbook, Del Research Coop., 1973.

Резюме

ЭКСПЕРИМЕНТАЛЬНОЕ ИССЛЕДОВАНИЕ РАЗРУШЕННЫХ РЕБЕР РАМ

Применены механика разрушения и эластооптические методы для определения поправочных функций интенсивности напряжений для разрушенных ребер рам. Представлен простой, инженерный метод анализа.

Streszczenie

DOŚWIADCZALNE BADANIE SPĘKANYCH NAROŻY RAM

Zastosowano mechanikę zniszczenia i metody elastooptyczne do określenia funkcji poprawkowych intensywności naprężeń dla spękanych naroży ram. Przedstawiono prostą, inżynierską metodę analizy.

INSTITUTE OF MECHANICS
and
INSTITUTE OF STATICS AND STRENGTH OF MATERIALS
TECHNICAL UNIVERSITY OF VIENNA, VIENNA, AUSTRIA.

Received August 31, 1982.